Appl. Phys. B (2013) 110:437–444
DOI 10.1007/s00340-012-5275-3

Applied Physics B
Lasers and Optics

Dose-controlled irradiation of cancer cells with laser-accelerated proton pulses

K. Zeil · M. Baumann · E. Beyreuther · T. Burris-Mog · T. E. Cowan · W. Enghardt · L. Karsch · S. D. Kraft · L. Laschinsky · J. Metzkes · D. Naumburger · M. Oppelt · C. Richter · R. Sauerbrey · M. Schürer · U. Schramm · J. Pawelke

Received: 9 November 2012 / Revised: 9 November 2012 / Published online: 25 November 2012

Abstract Proton beams are a promising tool for the improvement of radiotherapy of cancer, and compact laser-driven proton radiation (LDPR) is discussed as an alternative to established large-scale technology facilitating wider clinical use. Yet, clinical use of LDPR requires substantial development in reliable beam generation and transport, but also in dosimetric protocols as well as validation in radiobiological studies. Here, we present the first dose-controlled direct comparison of the radiobiological effectiveness of intense proton pulses from a laser-driven accelerator with conventionally generated continuous proton beams, demonstrating a first milestone in translational research. Controlled dose delivery, precisely online and offline monitored for each out of ~4,000 pulses, resulted in an unprecedented relative dose uncertainty of below 10 %, using approaches scalable to the next translational step toward radiotherapy application.

K. Zeil (✉) · M. Baumann · E. Beyreuther · T. Burris-Mog · T. E. Cowan · W. Enghardt · S. D. Kraft · J. Metzkes · M. Oppelt · C. Richter · R. Sauerbrey · U. Schramm · J. Pawelke
Helmholtz-Zentrum Dresden-Rossendorf (HZDR), Bautzner Landstraße 400, 01328 Dresden, Germany
e-mail: k.zeil@hzdr.de

M. Baumann · W. Enghardt · L. Karsch · L. Laschinsky · D. Naumburger · M. Oppelt · C. Richter · M. Schürer · J. Pawelke
OncoRay-National Center for Radiation Research in Oncology, TU Dresden, Fetscherstr. 74, 01307 Dresden, Germany

M. Baumann · W. Enghardt
Klinik für Strahlentherapie und Radioonkologie, Universitätsklinikum Carl Gustav Carus der TU Dresden, Fetscherstr. 74, 01307 Dresden, Germany

1 Introduction

Cancer represents the second highest cause of death in industrial societies. Today, at a steadily increasing rate, already more than 50 % of all cancer patients are treated with photon or electron radiotherapy during the course of their disease. Radiotherapy by protons or heavier ion beams, due to their inverse depth dose profile (Bragg peak), can achieve better physical dose distributions than the most modern photon therapy approaches. In the case of ions heavier than protons, the higher relative biological effectiveness (RBE) [1, 2] might be of additional therapeutic benefit. It is estimated that at least 10–20 % of all radiotherapy patients may benefit from proton or light ion therapy [3, 4] and indications are currently evaluated in clinical trials worldwide. Yet, making widespread use of this potential calls for very high levels of clinical expertise and quality control as well as for enormous economical investment and running costs associated with large-scale accelerator facilities. The former point is presently being addressed in clinical research with, e.g., advanced real-time motion compensation techniques, while the latter requires more compact and cost-effective, yet, equally reliable particle accelerators.

As a promising alternative to conventional proton sources, compact laser plasma based accelerators have been suggested [5–11]. Practically, LDPR originates from hydrogenated contaminants on almost any solid target surface when irradiated with sufficiently intense ultrashort-pulse laser light [12]. Electrons are heated to mega-electronvolt temperatures during the interaction, and driven out of the target volume. In the corresponding electric field, yielding unsurpassed gradients in the megavolt per micrometer range, protons at the surface efficiently gain initial energy [13]. Over the last decade, intense proton

pulses with energies exceeding several 10 MeV have been reached with large single-shot laser facilities. Yet, only with the recent generation of table-top 100 TW Ti:Sapphire lasers, operating at pulse repetition rates of up to 10 Hz, energies exceeding 10 MeV [14–18] became accessible for applications where also the average dose rate is of interest, e.g., for providing sufficiently short treatment durations of a few minutes. For the anticipated future application in radiation therapy, a further increase in the proton energy of up to 200–250 MeV is required, which is currently addressed by the investigation of novel acceleration schemes [19–21] as well as by ongoing laser development.

Equally indispensable for the development of devices suitable for radiobiological studies and clinical applications is the competitiveness of the laser plasma accelerator with conventional sources in terms of precision, reliability and reproducibility. Research in this field can adequately be performed with available technology and, in particular, presently accessible particle energies as introduced in Ref. [22]. The challenge is the development of a laser-based treatment facility taking into account the specific properties of LDPR, in particular, the comparatively broad energy spectrum and the distribution of the therapeutically required dose in a finite number of very intense pulses, where the level of the peak dose rate in one pulse can exceed the average by up to nine orders of magnitude. This task has to be addressed by translational research, meaning the transfer of the results of the complex and interdisciplinary basic research into clinical practice [23], starting from in vitro cell irradiation, over experiments with animals, to clinical studies. Vice versa the realization of each translational step represents a benchmark of the development status of the laser-driven dose-delivery system to a clinically applicable beam, being the main objective of our work.

In this sense, in this article, we directly compare the RBE of pulsed LDPR and conventionally accelerated continuous proton beams in vitro demonstrating scalable controlled dose-delivery and clinical precision standards for both sources. This work is building on previous work from our group [22] and the radiobiological results are consistent with first experiments performed by Yogo et al. [24, 25] and a recent single-pulse study of the RBE by Doria et al. [26] with retrospective dose evaluation.

2 Setup of the laser-driven proton dose-delivery system

The experiment was carried out with the ultra-short pulse Ti:Sapphire laser system Draco at HZDR [14], here providing an energy of 1.8 J on target contained in a pulse of 30-fs duration. When tightly focused onto a 2-µm-thick titanium foil target (Fig. 1), a peak intensity of $5 \times 10^{20}\,\mathrm{W/cm^2}$ can be achieved. All major parameters of the fully computer-controlled high-power laser system are monitored to provide for maximum stability. The proton radiation generated by the target-normal-sheath-acceleration mechanism [12] exhibits an exponential energy

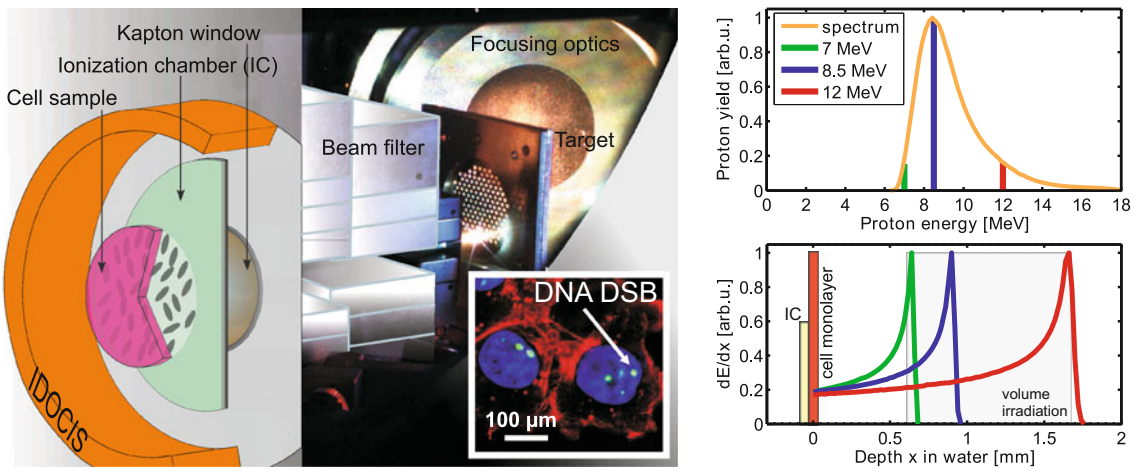

Fig. 1 *Left* Picture depicting the experimental setup for the irradiation of cell samples with LDPR at the instant of a laser shot. The laser pulse is focused by an off-axis parabolic mirror onto a thin target foil. Protons accelerated in the target normal sheath acceleration regime propagate through a magnetic filter and are transported to the irradiation site inside the air-filled integrated dosimetry and cell irradiation system (IDOCIS). The *bottom insert* shows a micrograph illustrating immunostained DNA double-strand breaks (DSB) in single-cell nuclei used to quantify radiation induced biological damage. *Right* The filtered proton energy spectrum at the position of the cell sample is shown. For representative energies of 7, 8.5, and 12 MeV, the normalized energy deposition in water is given as a function of the depth below. As illustrated, the cell monolayer is irradiated in the energy insensitive plateau region of the corresponding Bragg curves, well separated from the range of the energy dependent Bragg peaks, where volumetric sample irradiation would be performed

spectrum with a characteristic cutoff energy of up to 15 MeV. The remote-controlled target-alignment procedure ensures a high shot-to-shot reproducibility. A special target foil exchange device allows for about 1,000 shots without breaking the vacuum, sufficient to homogeneously irradiate about 40 cell samples with a dose of 2 Gy.

Directly behind the target the energetic protons pass through a magnetic dipole filter [27] applied to clean the pulse of all protons with energies below 8 MeV. Intrinsically, the direct line-of-sight between the interaction point and the irradiation site is blocked and thus secondary radiation generated in the laser plasma is suppressed. Downstream of the magnetic filter the integrated dosimetry and cell irradiation system (IDOCIS) is located [22, 28]. Its interior components for dosimetry and cell irradiation are separated from the vacuum of the target chamber by a thin plastic window. The IDOCIS module integrates a thin transmission ionization chamber for real-time control of dose delivery and a cell holder inset. The latter can be replaced by several reference dosimeters such as a Faraday cup (FC, design adopted from Ref. [29]), radiochromic films (RCF), or CR39 solid state nuclear track detectors to determine the applied 2D dose and spectral energy distribution in the plane of the cell monolayer. For that purpose, an absolute calibration for RCF and FC detectors was carried out before performing the irradiation experiments with laser-accelerated protons for proton energies of 5–60 MeV at the eye tumor therapy centre of the Helmholtz Zentrum Berlin (HZB), Germany [28]. The ionization chamber optimized for lowest ion energies, thus consisting of three metalized kapton foils (each only 7.5-μm thick), is permanently placed in front of the different insets and is used to establish the relationship between FC and RCF and to the real-time control of the dose delivery. It is therefore cross-calibrated to FC and RCF before and after each cell irradiation taking saturation effects at high dose rates into consideration (similar to Ref. [30]).

During the irradiation dose homogenization on a 2×6 mm^2 spot size is ensured by multiple rotations of the cell sample. The optimization and control of the homogenous 2D dose distribution in the plane of the cell monolayer and the estimation of the contribution of the inhomogeneity (below 5 %) to the dose error was performed with RCF and CR39 nuclear track detectors.

For the control of the dose deposited into the thin cell monolayer, the proton energy spectrum has to be known. Figure 1 (right) shows a typical normalized spectrum at the cell location deduced from Thomson parabola measurements recorded directly before the cell irradiation campaign and including the transmission of the energy selective beam delivery [22]. During the irradiation experiments, stacks of RCF and CR39, providing a coarse energy resolution due to the energy-range relationship of the stopping power, were used to cross-check the applied energy spectrum in the plane of the cell monolayer and complemented by the online observation of the stability of the spectral filtering with a plastic scintillator positioned between the dipole filter and the IDOCIS entrance pinhole.

In the presented experimental campaign, the use of sufficiently high proton energies at the cell layer position (>6.5 MeV) ensured a constant linear energy transfer (LET). Therefore, significantly less uncertainty in the energy-dependent energy loss was achieved than if the Bragg peak was be positioned at the depth of the cell monolayer. This method yields the most reliable exposure range for systematic studies as illustrated by the normalized energy deposition for the representative energies of 7, 8.5, and 12 MeV as a function of the depth in water depicted below the spectrum in Fig. 1.

3 Dose effect curves and dose uncertainty

For the irradiation experiment, the radiosensitive human squamous cell carcinoma cell line SKX was used [31]. Cells were seeded 1 day before irradiation on a thin biofilm as bottom of a chamber slide. The plating efficiency was in the range of 15–20 %. Before irradiation, 1 ml of cell culture medium was added, the well was closed with sterile parafilm and the sample was positioned in the horizontal LDPR beam. Further details on derivation, cultivation and handling of the cell line as well as applied sample geometries are provided in Refs. [22, 32, 33]. The cells were irradiated with a mean dose of 81 mGy per shot that corresponds to a peak dose rate for each proton bunch of 4×10^7 Gy/s. The dose was applied in the range between 0.5 and 4.3 Gy (0.43 Gy/min averaged over 1 min) and controlled by means of the ionization chamber in front of the cells.

The biological endpoint of the yield of residual DNA double-strand breaks (DSB) remaining 24 h after irradiation was analysed. It has been shown previously for this cell line that residual DNA DSB correlate closely with cell survival [34]. The DNA DSB were detected by means of fluorescent-labeled antibodies against the active forms of histone γ-H2AX [35] and protein 53BP1 [36]. Both molecules were activated and related to the position of radiation-induced DNA DSB [35, 36]. The average number of radiation-induced DNA DSB per cell nucleus was counted for each irradiated cell sample and evaluated as a function of the applied dose.

An in-house tandem Van-de-Graaf accelerator served as reference radiation source providing 7.2 MeV protons delivered as a continuous beam with a dose rate of 1.1 Gy/min in a homogeneous beam spot of 35 mm^2. The equipment and the dosimetry methods, e.g., including IDOCIS module and detectors, horizontal beam application, etc.,

were identical for both radiation sources (more details in Ref. [28]). As the irradiation setup was initially developed for the polychromatic beam of the laser plasma accelerator, no additional filtering was applied for the case of the monoenergetic tandem beam. For the dosimetry, the spectrum has no further implications, because the cell sample is positioned ahead of the Bragg peak (Fig. 1). Moreover, the location of both radiation sources and a cell laboratory on one site guarantees the direct comparability of radiobiological outcome for laser-driven and conventionally accelerated proton beams. To connect the successive experimental campaigns (LDPR and conventionally accelerated protons), and to identify possible deviations in the biological response arising from biological diversity, reference irradiations with standard 200-kV X-rays (filtered with 7 mm Be and 0.5 mm Cu) were performed in parallel to each proton experiment.

The dose effect curves of the laser-driven proton pulses (red dots) and the conventionally accelerated continuous proton beam (blue squares) are compared in Fig. 2. This direct comparison reveals no significant difference in the radiobiological effectiveness as indicated by the substantially overlapping confidence intervals (2σ) of the almost identical linearly fitted curves. Furthermore, a similar level of the relative dose error $\Delta D/D$ could be reached experimentally for both techniques and for each irradiated cell sample. As a major result, this level remains below 10 % as depicted in the inset of Fig. 2 and reaches the order of the clinical precision standard of 3–5 %.

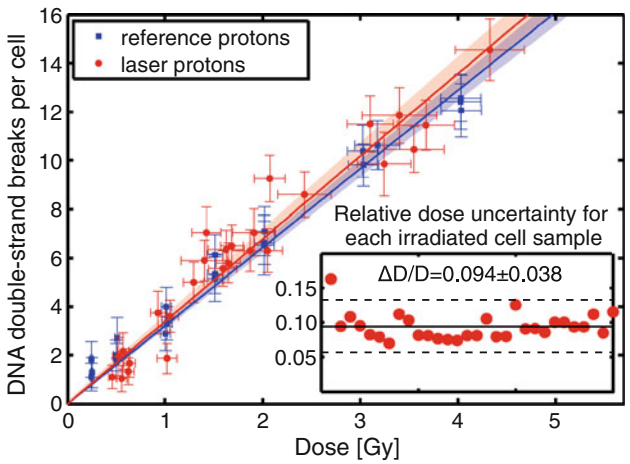

Fig. 2 The averaged number of DNA DSB plotted and linearly fitted as function of the applied dose for each cell sample irradiated with LDPR (*red*) in comparison with a continuous proton reference beam (*blue*). The *inset* shows the relative dose uncertainty for each sample irradiated with LDPR. The *error bars* on the biological measurements include all systematic errors caused by the used equipment, such as the scale uncertainty of pipettes and the automatic cell counting as well as statistical errors. The background of 0.96 ± 0.06 γ-H2AX foci per cell was determined using non-irradiated control samples and is already subtracted for each data point

The key to this with respect to LDPR unprecedented level of precision is the synergetic combination of first, the reduction of the uncertainty in the dose delivery caused by beam fluctuations and detector responses using two independent absolute dose formalisms, and second, the reliable operation of the laser-driven proton source based on well-controlled laser conditions on target.

The measurement of the precise dose applied to the cell monolayer is based on the implementation of radiochromic films and a Faraday cup into the irradiation site as two distinct, dose rate independent, and absolutely calibrated dosimetry systems. Using these systems, the absolute dose value and the relative dose uncertainty were determined for each irradiated cell sample individually by repeated cross-calibration of the real-time monitor signal of the transmission ionization chamber to RCF and FC directly before and after each irradiation. Performing a weighted average of the RCF and FC signals in combination with the use of sufficiently high proton energies at the cell monolayer position (>6.5 MeV) allowed for this significant reduction of the measurement uncertainty.

A sufficiently high shot-to-shot reproducibility of the proton pulses for the irradiation of single-cell samples could already be demonstrated at Draco in Ref. [22]. Further automation of the laser start-up protocol, monitoring, and the implementation of the target-alignment procedure extended this stability over a total operation period of 3 weeks comprising several thousands of shots. Long-term reliability was investigated by monitoring dedicated proton test pulses on 28 days out of 5 months. Dose and spectrum of these test pulses were measured with an RCF stack positioned 35 mm behind the target foil recording the complete unfiltered spatial proton energy distribution for single reference shots (Fig. 3). The pulse dose measured on the fifth film layer, corresponding to a reference depth of about 1 mm in water, and the characteristic cutoff value of the exponential proton energy spectrum (E_{max}), were used to characterize the proton beam. The overall average pulse dose of 5 ± 0.8 Gy and the overall average maximum proton energy 13.3 ± 0.6 MeV confirm reproducible system performance at the level required for radiobiological experiments over a period of 5 months.

This in principle allows for extending the experiments presented here to several tumor and normal tissue cell lines as well as to different biological endpoints as it is required to conclude on the RBE of pulsed LDPR for therapeutical applications. As an example, the clonogenic survival assay, commonly referred to as gold standard in radiotherapy-related research, was independently applied to few homogeneously irradiated probes. A comparison of the survival fraction of cells irradiated with LDPR and the continuous reference beam, using the same protocol as for the previous

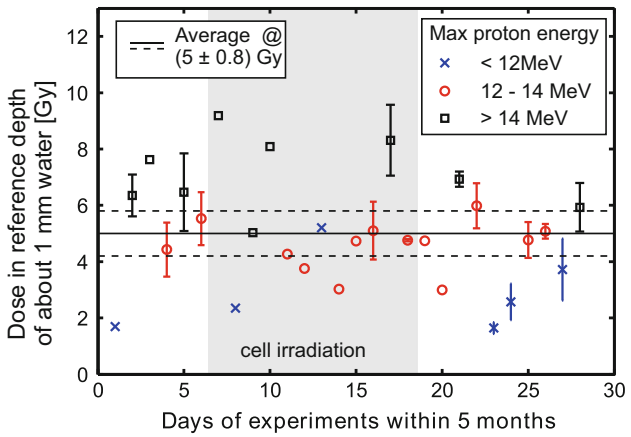

Fig. 3 Long-term stability of the test pulse dose evaluated for 28 days within 5 months (including the cell-irradiation experiment marked in *grey*). As the relevant parameter of the exponential spectrum the dose in a reference depth of about 1 mm water (this range requires an initial proton energy >10 MeV) is plotted, where all reference data collected on one experiment day are averaged. In addition, the characteristic proton cutoff energy (E_{max}) is coded into the colour of the data points

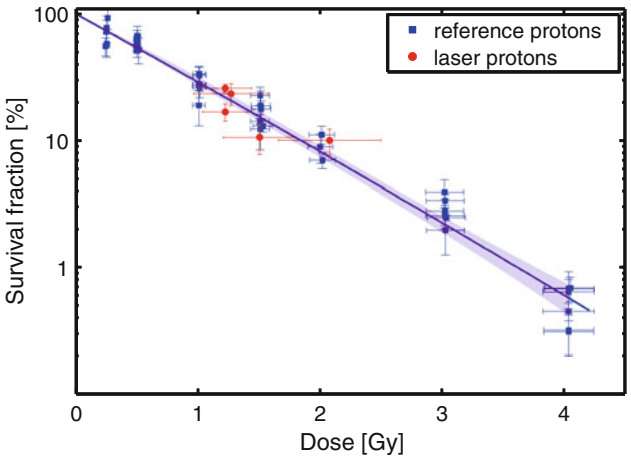

Fig. 4 The tumor cell survival (for cell line SKX) is depicted after irradiation with LDPR (*red*) and the reference proton beam (*blue*) determined using the clonogenic survival assay, as the gold standard in radiobiology. Here, the killing efficiency of the used radiation is measured by plating a certain number of cells after irradiation and counting the number of surviving colonies containing at least 50 cells after 13 days of incubation

study, is presented in Fig. 4. Again, no difference in the response to the beam properties is observed within the exemplarily investigated dose range.

4 Conclusions and outlook

Summarizing, laser-driven dose-delivery systems dedicated for the in vitro cell irradiation with proton pulses can be operated at a performance level that is sufficient for radiobiological studies on short as well as on long timescales and with a precise delivery of prescribed doses. Methods and components of the presented approach such as real-time transmission dose monitoring can be directly scaled to higher proton energies, later required for proton cancer therapy. This performance level has been validated by the independent measurement of two dose effect curves based on different endpoints.

Both radiobiological results are in good agreement with a complementary experiment performed at the Munich Tandem Van-de-Graaf accelerator [37, 38] and a recent study of the RBE of intense single pulses of LDPR, where the dose applied to the cells was varying across the probe and analyzed retrospectively for individual irradiated areas [26]. Making use of different pulse modes of the Tandem accelerator, the first study focused on the dependence of the RBE on the peak dose rate by comparing the effect of short-pulses (few nanoseconds) and continuous beams of 20 MeV protons, while the latter directly made use of the intrinsically high peak dose rates of LDPR of up to few Gy per pulse. It thus seems that all existing studies performed for different cell-lines and making use of different sources confirm that in the therapeutically relevant dose range of a few Gy, even if applied in a single pulse of only few nanoseconds duration, non-linear radiobiological effects due to simultaneous multiple damages in cells and, thus, below any timescale of repair mechanisms are unlikely to arise.

The next step in translational research will be the extension of the experiments to volume irradiation in animal experiments. In comparison to the studies on biological effects in two-dimensional cell monolayers, these experiments are more complex and require not only higher but also tunable proton energies.

Thus, to be able to proceed independently from the development of laser accelerators, an experimental setup is proposed in Fig. 5. The scheme relies on a refined combination of the techniques described above with an active energy selection filter and dedicated small tumors growing in the ear of mice close to the surface with a volume of about 1 mm^3. In previous measurements with the Draco laser system, the use of ultra-thin gold disks as targets, similar to the targets presented in Ref. [20], led to an increase in the measured dose per pulse by a factor of at least six in the proton energy range of interest (lower left Fig. 5) with respect to the titanium foil targets used for the dose effect curves in Fig. 2. Simultaneously, these targets enable high-precision alignment at high repetition rates due to lithographic technology-based fabrication.

In addition, the cell irradiation setup presented in Fig. 1 is extended by a pulsed solenoid providing a high capture and transport efficiency of up to 20–25 % measured in [39]. By tuning the delay between laser pulse and solenoid trigger in a multi-shot approach, the energy-dependent beam collimation allows for the active shaping of the

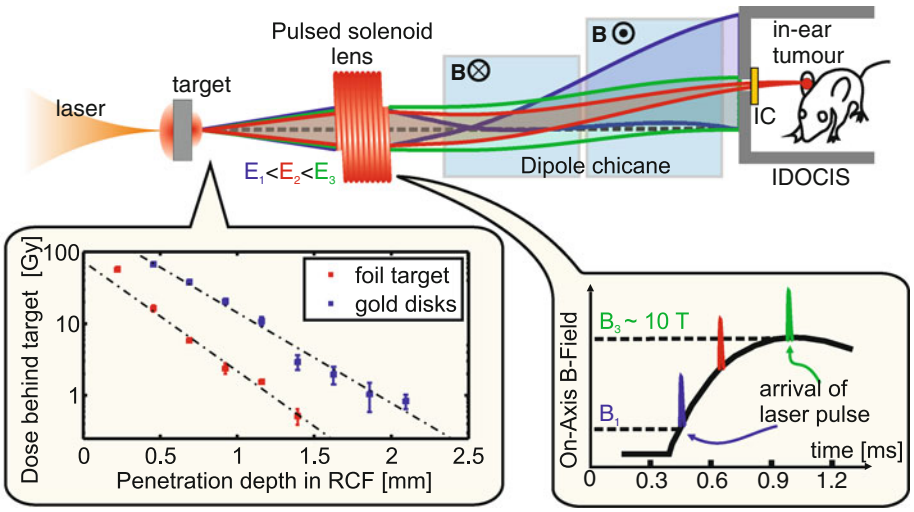

Fig. 5 Setup of the in vivo experiment to apply a homogeneous depth dose distribution to a tumor growing in the mouse ear ($\propto$1 mm^3). By the use of gold disk targets (around 100 µm in diameter and sub-micron thickness) the dose per pulse relative to standard planar foils is significantly increased as presented in the depth dose curves measured with RCF stacks 35 mm behind the target (average over 15 consecutive shots each). In addition, the presented cell-irradiation setup is extended by a pulsed solenoid to increase the transport efficiency and to ensure a homogeneous proton depth dose distribution in the tumor (c.f. Fig. 1). The generated polyenergetic divergent proton beam drifts through a pulsed magnetic solenoid lens [39]. By tuning the temporal delay of the laser pulse arrival relative to the current pulse driving the solenoid the proton energy spectrum can be actively shaped on a shot-to-shot basis as illustrated in the right box. The transmission of a certain proton energy ensemble ($E_1 < E_2 < E_3$) through the dipole chicane into the IDOCIS module is optimized according to the on-axis magnetic field (B_2 or B_1) at the moment the proton pulse passes the coil

spectral intensity of the proton energy spectrum given for the cell location in Fig. 1. Thus, a homogeneous proton depth dose distribution (spread-out Bragg peak) can be applied to the tumor without the need to shape the energy distribution in the plasma acceleration process.

The demonstrated advances in the performance of compact laser-driven proton sources and dedicated dosimetric techniques not only represent an important milestone on the way to the realization of a clinical laser-based proton treatment facility but also open the door to further applications where ultra-fast and reliable sources are required.

Acknowledgements The authors want to thank M. Sobiella, J. Woithe and Y. Dammene for the technical support and E. Lessmann for the work in the cell laboratory. We acknowledge S. Bock and U. Helbig for providing excellent laser support. The work has been supported by the German Federal Ministry of Education and Research (BMBF) under contract number 03ZIK445.

References

1. M. Durante, J.S. Loeffler, Charged particles in radiation oncology. Nature Rev. Clin. Oncol. **7**, 37–43 (2010)
2. D. Schardt, T. Elsässer, D. Schulz-Ertner, Heavy-ion tumor therapy: physical and radiobiological benefits. Rev. Mod. Phys. **82**, 383–425 (2010)
3. M.H. Baron, P. Pommier, V. Favrel, G. Truc, J. Balosso, J. Rochat, ETOILE project, A "One-day survey": as a reliable estimation of the potential recruitment for proton- and carbon-ion therapy in France. Radiother. Oncol. **73**, 15–17 (2004)
4. R. Mayer, U. Mock, R. Jager, R. Potter, C. Vutuc, H. Eiter, K. Krugmann, J. Hammer, B. Hirn, R. Hawliczek, T.H. Knocke-Abulesz, P. Lukas, E. Nechville, B. Pakisch, M. Papauschek, R. Wolfgang, W. Rhomberg, H. Sabitzer, A. Schratter-Sehn, S. Felix, I. Wedrich, T. Auberger, Epidemiological aspects of hadron therapy: a prospective nationwide study of the Austrian project MedAustron and the Austrian Society of Radiooncology (OEGRO). Radiother. Oncol. **73**, 24–28 (2004)
5. S.V. Bulanov, T.Z. Esirkepov, V.S. Khoroshkov, A.V. Kunetsov, F. Pegoraro, Oncological hadrontherapy with laser ion accelerators. Phys. Lett. A **99**, 240–247 (2002)
6. S.V. Bulanov, V.S. Khoroshkov, Feasibility of using laser ion accelerators in proton therapy. Plasma Phys. Rep. **28**, 453–456 (2002)
7. E. Fourkal, J.S. Li, M. Ding, T. Tajima, C.-M. Ma, Particle selection for laser-accelerated proton therapy feasibility study. Med. Phys. **30**, 1660–1670 (2003)
8. K.W.D. Ledingham, P. McKenna, R.P. Singhal, Applications for nuclear phenomena generated by ultra-intense lasers. Science **300**, 1107–1111 (2003)
9. V. Malka, S. Fritzler, E. Lefebvre, E. d'Humières, R. Ferrand, G. Grillon, C. Albaret, S. Meyroneinc, J.-P. Chambaret, A. Antonetti, D. Hulin, Practicability of protontherapy using compact laser systems. Medi. Phys. **31**, 1587–1592 (2004)
10. C.M. Ma, I. Veltchev, E. Fourkal, J.S. Li, W. Luo, J. Fan, T. Lin, A. Pollack, Development of a laser-driven proton accelerator for cancer therapy. Laser Phys. **16**, 639–646 (2006)
11. K.W.D. Ledingham, W. Galster, Laser-driven particle and photon beams and some applications. N. J. Phys. **12**, 045005 (2010)
12. S.C. Wilks, A.B. Langdon, T.E. Cowan, M. Roth, M. Singh, S. Hatchett, M.H. Key, D. Pennington, A. MacKinnon, R.A.

Snavely, Energetic proton generation in ultra-intense laser–solid interactions. Phys. Plasmas **8**, 542–549 (2001)
13. K. Zeil, J. Metzkes, T. Kluge, M. Bussmann, T.E. Cowan, S.D. Kraft, R. Sauerbrey, U. Schramm, Direct observation of prompt pre-thermal laser ion sheath acceleration. Nature Commun. **3**, 874 (2012)
14. K. Zeil, S.D. Kraft, S. Bock, M. Bussmann, T.E. Cowan, T. Kluge, J. Metzkes, T. Richter, R. Sauerbrey, U. Schramm, The scaling of proton energies in ultrashort pulse laser plasma acceleration. N. J. Phys. **12**, 045015 (2010)
15. F. Dollar, T. Matsuoka, G.M. Petrov, A.G.R. Thomas, S.S. Bulanov, V. Chvykov, J. Davis, G. Kalinchenko, C. McGuffey, L. Willingale, V. Yanovsky, A. Maksimchuk, K. Krushelnick, Control of energy spread and dark current in proton and ion beams generated in high-contrast laser solid interactions. Phys. Rev. Lett. **107**, 065003 (2011)
16. A. Henig, S. Steinke, M. Schnürer, T. Sokollik, R. Hörlein, D. Kiefer, D. Jung, J. Schreiber, B.M. Hegelich, X.Q. Yan, J. Meyer-ter Vehn, T. Tajima, P.V. Nickles, W. Sandner, D. Habs, Radiation-pressure acceleration of ion beams driven by circularly polarized laser pulses. Phys. Rev. Lett. **103**, 245003 (2009)
17. R. Prasad, S. Ter-Avetisyan, D. Doria, K.E. Quinn, L. Romagnani, P.S. Foster, C.M. Brenner, J.S. Green, P. Gallegos, M.J.V. Streeter, D.C. Carroll, O. Tresca, N.P. Dover, C.A.J. Palmer, J. Schreiber, D. Neely, Z. Najmudin, P. McKenna, M. Zepf, M. Borghesi, Proton acceleration using 50 fs, high intensity astra-gemini laser pulses. Nucl. Instrum. Methods Phys. Res. Sect. A Accel. Spectrom. Detect. Assoc. Equip. **653**, 113–115 (2011)
18. K. Ogura, M. Nishiuchi, A.S. Pirozhkov, T. Tanimoto, A. Sagisaka, T. Zh. Esirkepov, M. Kando, T. Shizuma, T. Hayakawa, H. Kiriyama, T. Shimomura, S. Kondo, S. Kanazawa, Y. Nakai, H. Sasao, F. Sasao, Y. Fukuda, H. Sakaki, M. Kanasaki, A. Yogo, S.V. Bulanov, P.R. Bolton, K. Kondo, Proton acceleration to 40 MeV using a high intensity, high contrast optical parametric chirped-pulse amplification/Ti:sapphire hybrid laser system. Opt. Lett. **37**, 2868–2870 (2012)
19. C.A.J. Palmer, N.P. Dover, I. Pogorelsky, M. Babzien, G.I. Dudnikova, M. Ispiriyan, M.N. Polyanskiy, J. Schreiber, P. Shkolnikov, V. Yakimenko, Z. Najmudin, Monoenergetic proton beams accelerated by a radiation pressure driven shock. Phys. Rev. Lett. **106**, 014801 (2011)
20. S. Buffechoux, J. Psikal, M. Nakatsutsumi, L. Romagnani, A. Andreev, K. Zeil, M. Amin, P. Antici, T. Burris-Mog, A. Compant-La-Fontaine, E. d'Humières, S. Fourmaux, S. Gaillard, F. Gobet, F. Hannachi, S. Kraft, A. Mancic, C. Plaisir, G. Sarri, M. Tarisien, T. Toncian, U. Schramm, M. Tampo, P. Audebert, O. Willi, T.E. Cowan, H. Pépin, V. Tikhonchuk, M. Borghesi, J. Fuchs, Hot electrons transverse refluxing in ultraintense laser-solid interactions. Phys. Rev. Lett. **105**, 015005 (2010)
21. S.A. Gaillard, T. Kluge, K.A. Flippo, M. Bussmann, B. Gall, T. Lockard, M. Geissel, D.T. Offermann, M. Schollmeier, Y. Sentoku, T.E. Cowan, Increased laser-accelerated proton energies via direct laser-light-pressure acceleration of electrons in microcone targets. Phys. Plasmas **18**, 056710 (2011)
22. S.D. Kraft, C. Richter, K. Zeil, M. Baumann, E. Beyreuther, S. Bock, M. Bussmann, T.E. Cowan, Y. Dammene, W. Enghardt, U. Helbig, L. Karsch, T. Kluge, L. Laschinsky, E. Lessmann, J. Metzkes, D. Naumburger, R. Sauerbrey, M. Schürer, M. Sobiella, J. Woithe, U. Schramm, J. Pawelke, Dose-dependent biological damage of tumour cells by laser-accelerated proton beams. N. J. Phys. **12**, 085003 (2010)
23. M. Baumann, S.M. Bentzen, W. Doerr, M.C. Joiner, M. Saunders, I.F. Tannock, H.D. Thames. The translational research chain: is it delivering the goods? Int. J. Radiat. Oncol. Biol. Phys. **49**,345–351 (2001)
24. A. Yogo, K. Sato, M. Nishikino, M. Mori, T. Teshima, H. Numasaki, M. Murakami, Y. Demizu, S. Akagi, S. Nagayama, K. Ogura, A. Sagisaka, S. Orimo, M. Nishiuchi, A.S. Pirozhkov, M. Ikegami, M. Tampo, H. Sakaki, M. Suzuki, I. Daito, Y. Oishi, H. Sugiyama, H. Kiriyama, H. Okada, S. Kanazawa, S. Kondo, T. Shimomura, Y. Nakai, M. Tanoue, H. Sasao, D. Wakai, P.R. Bolton, H. Daido, Application of laser-accelerated protons to the demonstration of DNA double-strand breaks in human cancer cells. Appl. Phys. Lett. **94**, 181502 (2009)
25. A. Yogo, T. Maeda, T. Hori, H. Sakaki, K. Ogura, M. Nishiuchi, A. Sagisaka, H. Kiriyama, H. Okada, S. Kanazawa, T. Shimomura, Y. Nakai, M. Tanoue, F. Sasao, P.R. Bolton, M. Murakami, T. Nomura, S. Kawanishi, K. Kondo, Measurement of relative biological effectiveness of protons in human cancer cells using a laser-driven quasimonoenergetic proton beamline. Appl. Phys. Lett. **98**, 053701 (2011)
26. D. Doria, K.F. Kakolee, S. Kar, S.K. Litt, F. Fiorini, H. Ahmed, S. Green, J.C.G. Jeynes, J. Kavanagh, D. Kirby, K.J. Kirkby, C.L. Lewis, M.J. Merchant, G. Nersisyan, R. Prasad, K.M. Prise, G. Schettino, M. Zepf, M. Borghesi. Biological effectiveness on live cells of laser driven protons at dose rates exceeding 10^9 Gy/s. AIP **2**, 011209 (2012)
27. J. Metzkes, T.E. Cowan, L. Karsch, S.D. Kraft, J. Pawelke, C. Richter, T. Richter, K. Zeil, U. Schramm, Preparation of laser-accelerated proton beams for radiobiological applications. Nucl. Instrum. Methods Phys. Res. Sect. A Accel. Spectrom. Detect. Assoc. Equip. **653**, 172–175 (2011)
28. C. Richter, L. Karsch, Y. Dammene, S.D. Kraft, J. Metzkes, U. Schramm, M. Schürer, M. Sobiella, A. Weber, K. Zeil, J. Pawelke, A dosimetric system for quantitative cell irradiation experiments with laser-accelerated protons. Phys. Med. Biol. **56**, 1529 (2011)
29. R. Cambria, J. Hérault, N. Brassart, M. Silari, P. Chauvel, Proton beam dosimetry: a comparison between the faraday cup and an ionization chamber. Phys. Med. Biol. **42**, 1185 (1997)
30. L. Karsch, C. Richter, J. Pawelke, Experimental investigation of the collection efficiency of a PTW Roos ionization chamber irradiated with pulsed beams at high pulse dose with different pulse lengths. Zeitschrift für Medizinische Physik **21**, 4–10 (2011)
31. U. Kasten-Pisula, A. Menegakis, I. Brammer, K. Borgmann, W.Y. Mansour, S. Degenhardt, M. Krause, A. Schreiber, J. Dahm-Daphi, C. Petersen, E. Dikomey, M. Baumann, The extreme radiosensitivity of the squamous cell carcinoma SKX is due to a defect in double-strand break repair. Radiother. Oncol. **90**, 257–264 (2009)
32. E. Beyreuther, E. Lessmann, J. Pawelke, S. Pieck, DNA double strand breaks signaling: X-ray energy dependence residual co-localised foci of γ-H2AX and 53BP1. Int. J. Radiat. Biol. **85**, 1042–1050 (2009)
33. L. Laschinsky, M. Baumann, E. Beyreuther, W. Enghardt, M. Kaluza, L. Karsch, E. Lessmann, D. Naumburger, M. Nicolai, C. Richter, R. Sauerbrey, H.P. Schlenvoigt, J. Pawelke, Radiobiological effectiveness of laser accelerated electrons in comparison to electron beams from a conventional linear accelerator. J. Radiat. Res. **53**, 395–403 (2012)
34. A. Menegakis, A. Yaromina, W. Eicheler, A. Dörfler, B. Beuthien-Baumann, H.D. Thames, M. Baumann, M. Krause, Prediction of clonogenic cell survival curves based on the number of residual DNA double strand breaks measured by γH2AX staining. nt. J. Radiat. Biol. **85**, 1032–1041 (2009)
35. E.P. Rogakou, D.R. Pilch, A.H. Orr, V.S. Ivanova, W.M. Bonner, DNA Double-stranded Breaks Induce Histone H2AX Phosphorylation on Serine 139. J. Biol. Chem. **273**, 5858–5868 (1998)
36. I. Rappold, K. Iwabuchi, T. Date, J. Chen, Tumor Suppressor P53 Binding Protein 1 (53bp1) Is Involved in DNA Damage Signaling Pathways. J. Cell Biol. **153**, 613–620 (2001)

37. T.E. Schmid, G. Dollinger, A. Hauptner, V. Hable, C. Greubel, S. Auer, A.A. Friedl, M. Molls, B. Röper, No Evidence for a Different RBE between Pulsed and Continuous 20 MeV Protons. Radiat. Res. **172**, 567–574 (2009)
38. O. Zlobinskaya, G. Dollinger, D. Michalski, V. Hable, C. Greubel, G. Du, G. Multhoff, B. Röper, M. Molls, T. Schmid, Induction and repair of DNA double-strand breaks assessed by gamma-H2AX foci after irradiation with pulsed or continuous proton beams. Radiat. Environ. Biophys. **51**, 23–32 (2012)
39. T. Burris-Mog, K. Harres, F. Nürnberg, S. Busold, M. Bussmann, O. Deppert, G. Hoffmeister, M. Joost, M. Sobiella, A. Tauschwitz, B. Zielbauer, V. Bagnoud, T. Herrmannsdoerfer, M. Roth, T.E. Cowan, Laser accelerated protons captured and transported by a pulse power solenoid. Phys. Rev. Special Top. Accel. Beams **14**, 121301 (2011)